United States Department of Commerce
Technology Administration
National Institute of Standards and Technology

NIST Technical Note 1384

Dielectric Measurements Using a Reentrant Cavity: Mode-Matching Analysis

James Baker-Jarvis
Bill F. Riddle

NIST Technical Note 1384

Dielectric Measurements Using a Reentrant Cavity: Mode-Matching Analysis

James Baker-Jarvis
Bill F. Riddle

Electromagnetic Fields Division
Electronics and Electrical Engineering Laboratory
National Institute of Standards and Technology
325 Broadway
Boulder, Colorado 80303-3328

November 1996

U.S. DEPARTMENT OF COMMERCE, Michael Kantor, Secretary
TECHNOLOGY ADMINISTRATION, Mary L. Good, Under Secretary for Technology
NATIONAL INSTITUTE OF STANDARDS AND TECHNOLOGY, Arati Prabhakar, Director

National Institute of Standards and Technology Technical Note
Natl. Inst. Stand. Technol., Tech. Note 1384, 16 pages (November 1996)
CODEN:NTNOEF

U.S. GOVERNMENT PRINTING OFFICE
WASHINGTON: 1996

For sale by the Superintendent of Documents, U.S. Government Printing Office, Washington, DC 20402-9325

Dielectric Measurements Using a Reentrant Cavity: Mode-Matching Analysis

James Baker-Jarvis and Bill F. Riddle

Electromagnetic Fields Division, National Institute of Standards and Technology, Boulder, CO 80303-3328

Abstract

The coaxial reentrant cavity dielectric measurement technique is examined. A full-mode model for the cavity is developed and solved numerically. Analytical expressions for wall losses are presented. The filling factor due to a partially-filled cavity is discussed. Dielectric results are presented and compare very closely to previous round-robin results.

Key words: cavity; coaxial; dielectric constant; loss factor; microwave measurements; permeability measurement; permittivity measurement; reentrant; resonant

1. Introduction

In this report we develop the theory underlying the reentrant-cavity dielectric measurement technique. A full-mode model for the cavity is developed and solved numerically. Analytical expressions for reentrant-cavity characterization are presented.

Many radio-frequency applications require an accurate value of the component of the permittivity normal to the plane of the material. The reentrant cavity is unique since it is possible to accurately measure materials at frequencies from 100 MHz to 1 GHz with axial electric field [1, 2]. The reentrant cavity consists of a coaxial line or other transmission line with end walls, and a gap in the inner electrode where a sample is positioned. If the gap is at either end of the cavity, then the system is a *singly reentrant cavity*; otherwise it is a *doubly reentrant cavity*. The doubly reentrant cavity has a stronger electric field in the gap than the singly reentrant cavity and

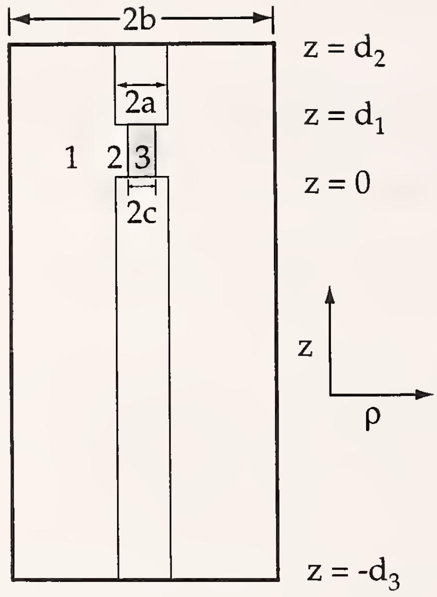

Figure 1: The reentrant cavity with regions 1, 2, and 3 denoted. The coaxial line inner and outer diameters 2a and 2b, and sample diameter 2c are indicated in the figure.

is more useful for permittivity determination. Applications include measurements of substrates, circuit boards, printed-wiring boards, and bulk materials.

Two approaches have been used for modeling the reentrant cavity. The first is a lumped-circuit approximation [1, 2]. The other approach, which we develop in detail, is a rigorous mode-matching technique [3-5]. Our approach differs from previous work in that we develop the full mode-matched solution for the doubly reentrant cavity and present the details of the calculations.

2. Mode-Matching Theory

The reentrant cavity method can be used to measure either permittivity or permeability. Permeability is most accurately measured by placing the sample in the strong magnetic field near an end plate. Permittivity is most accurately measured in a region of strong electric field, such as in a gap in the center conductor away from the end plates. We will restrict our analysis to permittivity determination; however, the equations are valid for arbitrary permeability. The material under test is assumed to have permittivity of $\epsilon_s^* = [\epsilon_r' - j\epsilon_r'']\epsilon_o = \epsilon_r^*\epsilon_o$ and permeability $\mu_s^* = [\mu_r' - j\mu_r'']\mu_o = \mu_r^*\mu_o$, where ϵ_o and μ_o are the permittivity and permeability of vacuum. The dimensions of the cavity are shown in figure 1. The coaxial sections have inner and outer radii a and b, respectively. The sample has radius c, which may be smaller than the inner conductor radius. The sample thickness is d_1. In the mode-matching technique the frequency

$$\omega = \omega_r + j\omega_r/2Q, \tag{1}$$

where ω_r is the measured resonant frequency and Q is the quality factor is complex.

We assume that only TM_{0m} modes are excited in the cavity. The TEM mode is excluded because of the gap in the center conductor. The fields can be derived from either H_ϕ or E_z in all regions. The magnetic field satisfies the vector Helmholtz equation

$$\nabla^2 \vec{H} + k^2 \vec{H} = 0. \tag{2}$$

Symmetry requires that only an azimuthal magnetic field is excited. H_ϕ satisfies

$$[\frac{\partial^2}{\partial \rho^2} + \frac{1}{\rho}\frac{\partial}{\partial \rho} - \frac{1}{\rho^2} + \frac{\partial^2}{\partial z^2} + k_i^2]H_{\phi(i)}(\rho, z) = 0 \tag{3}$$

in regions where $i = 1, 2,$ or 3, $k_i^2 = \omega^2 \epsilon_{ri}^* \mu_{ri}^* / c_v^2$, and c_v is the speed of light relative to vacuum. The electric field components are E_z and E_ρ.

The boundary conditions on the fields are

$$\begin{aligned}
E_z(a, z) &= 0, \quad (d_2 > z > d_1, \ 0 > z > -d_3), \\
E_z(b, z) &= 0, \quad (d_2 > z > -d_3), \\
E_\rho(\rho, d_2) &= E_\rho(\rho, -d_3) = 0, \quad (a < \rho < b), \\
E_\rho(\rho, d_1) &= E_\rho(\rho, 0) = 0, \quad (0 < \rho < a), \\
E_z(a^{(+)}, z) &= E_z(a^{(-)}, z), \quad (0 < z < d_1), \\
H_\phi(c^{(+)}, z) &= H_\phi(c^{(-)}, z), \quad (0 < z < d_1), \\
H_\phi(a^{(+)}, z) &= H_\phi(a^{(-)}, z), \quad (0 < z < d_1), \\
E_z(c^{(+)}, z) &= E_z(c^{(-)}, z), \quad (0 < z < d_1).
\end{aligned} \tag{4}$$

The boundary-value problem defined in eqs (3) and (4) can be shown to be unique.

2.1. Fields

In this section we develop expressions for TM_{0n} field structure in the reentrant cavity. The electric field has components E_ρ and E_z, and the magnetic field has component H_ϕ. The general solution can be written in the form

$$H_{\phi(i)}(\rho, z) = \sum_n A_{n(i)} R_{n(i)}(\rho) f_{n(i)}(z). \tag{5}$$

The eigenfunctions satisfy

$$\frac{d^2 f_n(z)}{dz^2} = -\lambda_n^2 f_n(z). \tag{6}$$

Since we require E_ρ to vanish at $z = -d_3$ and $z = d_2$ we must have

$$\frac{df_n}{dz}(z = d_2) = \frac{df_n}{dz}(z = -d_3) = 0; \tag{7}$$

therefore in region 1

$$f_{n(1)}(z) = \cos\left((d_2 - z)n\pi/L\right), \tag{8}$$

where $L = d_2 + d_3$ and $n = 0, 1, 2...$ In regions 2 and 3, the eigenfunctions satisfy eq (6) with the same boundary conditions, but on the ends of the inner conductor instead of on the cavity endplates. In regions 2 and 3,

$$f_{n(2)}(z) = \cos\left(n\pi z/d_1\right). \tag{9}$$

The magnetic field in region 1 is

$$H_{\phi(1)}(\rho, z) = -\sum_{m=0}^{\infty} A_{m(1)} \frac{j\omega\epsilon_1^*}{\sqrt{k_1^2 - (m\pi/L)^2}} [J_1(\sqrt{k_1^2 - (m\pi/L)^2}\rho) + Q_{1m} N_1(\sqrt{k_1^2 - (m\pi/L)^2}\rho)] \times \cos\left((d_2 - z)m\pi/L\right). \tag{10}$$

J_1, N_1, J_0, and N_0 are Bessel functions of complex argument. Equation (10) is written in a form to be consistent with previous publications [3]. The other field components can be generated by

$$E_\rho = -\frac{1}{j\omega\epsilon^*}\frac{\partial H_\phi}{\partial z}, \tag{11}$$

$$E_z = \frac{1}{j\omega\epsilon^*}\frac{1}{\rho}\frac{\partial(\rho H_\phi)}{\partial\rho}. \tag{12}$$

These are

$$E_{\rho(1)}(\rho, z) = \sum_{m=1}^{\infty} A_{m(1)} \frac{(m\pi/L)}{\sqrt{k_1^2 - (m\pi/L)^2}} [J_1(\sqrt{k_1^2 - (m\pi/L)^2}\rho) + Q_{1m} N_1(\sqrt{k_1^2 - (m\pi/L)^2}\rho)] \times \sin\left((d_2 - z)m\pi/L\right), \tag{13}$$

$$E_{z(1)}(\rho, z) = -\sum_{m=0}^{\infty} A_{m(1)} [J_0(\sqrt{k_1^2 - (m\pi/L)^2}\rho) + Q_{1m} N_0(\sqrt{k_1^2 - (m\pi/L)^2}\rho)] \times \cos\left(m\pi(d_2 - z)/L\right). \tag{14}$$

The condition that E_ρ vanishes on the outer conductor requires

$$Q_{1m} = -\frac{J_0(\sqrt{k_1^2 - (m\pi/L)^2}b)}{N_0(\sqrt{k_1^2 - (m\pi/L)^2}b)}. \tag{15}$$

In region 2, the fields are

$$E_{z(2)}(\rho, z) = -\sum_{m=0}^{\infty} A_{m(2)}[J_0(\sqrt{k_2^2 - (m\pi/d_1)^2}\rho)$$
$$+Q_{2m}N_0(\sqrt{k_2^2 - (m\pi/d_1)^2}\rho)]\cos(m\pi z/d_1), \tag{16}$$

$$E_{\rho(2)}(\rho, z) = \sum_{m=1}^{\infty} A_{m(2)}\frac{(m\pi/d_1)}{\sqrt{k_2^2 - (m\pi/d_1)^2}}[J_1(\sqrt{k_2^2 - (m\pi/d_1)^2}\rho)$$
$$+Q_{2m}N_1(\sqrt{k_2^2 - (m\pi/d_1)^2}\rho)]\sin(m\pi z/d_1), \tag{17}$$

$$H_{\phi(2)}(\rho, z) = -\sum_{m=0}^{\infty} A_{m(2)}\frac{j\omega\epsilon_2^*}{\sqrt{k_2^2 - (m\pi/d_1)^2}}[J_1(\sqrt{k_2^2 - (m\pi/d_1)^2}\rho)$$
$$+Q_{2m}N_1(\sqrt{k_2^2 - (m\pi/d_1)^2}\rho)]\cos(m\pi z/d_1). \tag{18}$$

In region 3, where the sample resides, the fields are

$$E_{z(3)}(\rho, z) = -\sum_{m=0}^{\infty} A_{m(3)}J_0(\sqrt{k_3^2 - (m\pi/d_1)^2}\rho)\cos(m\pi z/d_1), \tag{19}$$

$$E_{\rho(3)}(\rho, z) = \sum_{m=1}^{\infty} A_{m(3)}\frac{(m\pi/d_1)}{\sqrt{k_3^2 - (m\pi/d_1)^2}}J_1(\sqrt{k_3^2 - (m\pi/d_1)^2}\rho)\sin(m\pi z/d_1), \tag{20}$$

$$H_{\phi(3)}(\rho, z)$$
$$= -\sum_{m=0}^{\infty} A_{m(3)}\frac{j\omega\epsilon_3^*}{\sqrt{k_3^2 - (m\pi/d_1)^2}}J_1(\sqrt{k_3^2 - (m\pi/d_1)^2}\rho)\cos(m\pi z/d_1). \tag{21}$$

2.2. Matching between Regions

If we equate expansions for H_ϕ between regions 1 and 2, at $\rho = a$ in eqs (10) and (18), multiply each side by an axial eigenfunction, and integrate over $[0, d_1]$, we obtain the following system of equations

$$\frac{d_1}{2}(1+\delta_{n0})A_{n(2)}\frac{\epsilon_2^*}{\sqrt{k_2^2-(n\pi/d_1)^2}}[J_1(\sqrt{k_2^2-(n\pi/d_1)^2}a)+Q_{2n}N_1(\sqrt{k_2^2-(n\pi/d_1)^2}a)] \tag{22}$$

$$= \sum_{m=0}^{\infty} A_{m(1)}B_{mn}\frac{\epsilon_1^*}{\sqrt{k_1^2-(m\pi/L)^2}}[J_1(\sqrt{k_1^2-(m\pi/L)^2}a)+Q_{1m}N_1(\sqrt{k_1^2-(m\pi/L)^2}a)]. \tag{23}$$

Equation 23 may be rearranged and expressed in vector form

$$\vec{A}_2 = \mathbf{L_5}\vec{A}_1, \tag{24}$$

where

$$\mathbf{L}_{5mn} = \frac{B_{mn}\frac{\epsilon_1^*}{\sqrt{k_1^2-(m\pi/L)^2}}[J_1(\sqrt{k_1^2-(m\pi/L)^2}a)+Q_{1m}N_1(\sqrt{k_1^2-(m\pi/L)^2}a)]}{\frac{d_1}{2}(1+\delta_{n0})\frac{\epsilon_2^*}{\sqrt{k_2^2-(n\pi/d_1)^2}}[J_1(\sqrt{k_2^2-(n\pi/d_1)^2}a)+Q_{2n}N_1(\sqrt{k_2^2-(n\pi/d_1)^2}a)]}. \tag{25}$$

Similarly, if we equate eqs (14) and (16) between regions 1 and 2, multiply each side by an axial eigenfunction, and integrate over $[-d_3, d_2]$, we obtain

$$\frac{L}{2}(1+\delta_{n0})A_{n(1)}[J_0(\sqrt{k_1^2-(n\pi/L)^2}a)+Q_{1n}N_0(\sqrt{k_1^2-(n\pi/L)^2}a)]$$
$$= \sum_{m=0}^{\infty} A_{m(2)}B_{mn}[J_0(\sqrt{k_2^2-(m\pi/d_1)^2}a)+Q_{2m}N_0(\sqrt{k_2^2-(m\pi/d_1)^2}a)], \tag{26}$$

or

$$\vec{A}_1 = \mathbf{L_6}\vec{A}_2, \tag{27}$$

where

$$\mathbf{L}_{6mn} = \frac{B_{mn}[J_0(\sqrt{k_2^2-(m\pi/d_1)^2}a)+Q_{2m}N_0(\sqrt{k_2^2-(m\pi/d_1)^2}a)]}{\frac{L}{2}(1+\delta_{n0})[J_0(\sqrt{k_1^2-(n\pi/L)^2}a)+Q_{1n}N_0(\sqrt{k_1^2-(n\pi/L)^2}a)]}. \tag{28}$$

Requiring this integration to be 0 over $d_1 < z < d_2$ and $-d_3 < z < 0$ incorporates the boundary condition $E_z = 0$ on the inner conductor.

The coefficients B_{mn} can be calculated analytically. For $n = m$, $B_{mn} = d_1$, otherwise

$$\begin{aligned} B_{mn} &= \int_0^{d_1} \cos(n\pi z/d_1)\cos(m\pi(d_2 - z)/L)dz \\ &= \frac{d_1 L \sin(\pi(\frac{d_1 m}{L} - \frac{d_2 m}{L} + n))}{2\pi(d_1 m + Ln)} + \frac{d_1 L \sin(\pi(\frac{d_1 m}{L} - \frac{d_2 m}{L} - n))}{2\pi(d_1 m - Ln)} \\ &+ \frac{d_1^2 Lm}{\pi(d_1 m - Ln)(d_1 m + Ln)} \sin(\pi d_2 m/L). \end{aligned} \tag{29}$$

Since the modal fields decouple between regions 2 and 3 at $\rho = c$, we can write

$$A_{m(2)}[J_0(\sqrt{k_2^2 - (m\pi/d_1)^2}c) + Q_{2m}N_0(\sqrt{k_2^2 - (m\pi/d_1)^2}c)] = A_{m(3)}J_0(\sqrt{k_3^2 - (m\pi/d_1)^2}c), \tag{30}$$

and therefore,

$$\begin{aligned} & A_{m(3)} \frac{\epsilon_3^* \sqrt{k_2^2 - (m\pi/d_1)^2}}{\epsilon_2^* \sqrt{k_3^2 - (m\pi/d_1)^2}} J_1(\sqrt{k_3^2 - (m\pi/d_1)^2}c) \\ &= A_{m(2)}[J_1(\sqrt{k_2^2 - (m\pi/d_1)^2}c) + Q_{2m}N_1(\sqrt{k_2^2 - (m\pi/d_1)^2}c)]. \end{aligned} \tag{31}$$

We can determine the coefficients Q_{2m} from eqs (30) and (31)

$$Q_{2m} = \frac{ZJ_0(\sqrt{k_2^2 - (m\pi/d_1)^2}c) - J_1(\sqrt{k_2^2 - (m\pi/d_1)^2}c)}{N_1(\sqrt{k_2^2 - (m\pi/d_1)^2}c) - ZN_0(\sqrt{k_2^2 - (m\pi/d_1)^2}c)}, \tag{32}$$

where

$$Z = \frac{\epsilon_3^* \sqrt{k_2^2 - (m\pi/d_1)^2} J_1(\sqrt{k_3^2 - (m\pi/d_1)^2}c)]}{\epsilon_2^* \sqrt{k_3^2 - (m\pi/d_1)^2} J_0(\sqrt{k_3^2 - (m\pi/d_1)^2}c)}. \tag{33}$$

Equations (24) and (27) can be combined to form

$$\vec{A_2} = \mathbf{L_5 L_6} \vec{A_2}. \tag{34}$$

In order to have a nontrivial solution to this homogeneous system of equations, the determinant of the coefficients

$$\det(\mathbf{I} - \mathbf{L_5 L_6}) = 0, \tag{35}$$

must vanish. Equation (35) yields ϵ_3^*, given complex resonant frequency and quality factor. There are many roots to the equation, but use of an accurate initial guess allows convergence to the correct solution. Alternatively, given ϵ_3^*, the complex resonant frequency can be determined.

The matrices $\mathbf{L}_5$ and $\mathbf{L}_6$ have infinite dimension. In calculations, the matrices must be truncated. Numerical calculation shows that in regions 2 and 3, only 2 to 4 eigenfunctions are required since the fields are strongly evanescent. This can be seen by examination of the argument of the Bessel function in region 3, $\sqrt{k_3^2 - (m\pi/d_1)^2}$. Since d_1 is usually only a few millimeters, this quantity has a large imaginary component which produces a strong damping. In region 1, since the dimensions are larger, there is less damping, and more eigenfunctions are required to obtain a converged solution. In region 1, 20 to 90 eigenfunctions are required for accurate calculation of permittivity.

3. Cavity Losses

In this section we summarize the theory for calculation of dielectric losses in the reentrant cavity [4]. Losses in cavities originate from imperfectly conducting walls, sample loss, and coupling port losses. The analysis of cavity loss is more complicated than the analysis of the empty cavity when the cavity is partially filled with material.

In the time domain, the electric fields in a lossy cavity are of the form

$$\vec{E} \approx \exp(j\omega t - \alpha t)\vec{E}_0, \tag{36}$$

where α is an attenuation factor due to dielectric, coupling port, and cavity wall losses.

The stored electric and magnetic energy in a cavity is

$$U_{se} = \frac{1}{4} Re \int \vec{D} \cdot \vec{E} dV, \tag{37}$$

$$U_{sm} = \frac{1}{4} Re \int \vec{B} \cdot \vec{H} dV. \tag{38}$$

Since the stored electric and magnetic energies are equal at resonance,

$$U_{se} = \int \frac{\epsilon_r' \epsilon_0}{4} |\vec{E}|^2 dV = \int \frac{\mu_r' \mu_0}{4} |\vec{H}|^2 dV = U_{sm}. \tag{39}$$

Therefore the total stored energy in a cavity is

$$U_s = 2U_{se} = 2U_{sm}. \tag{40}$$

The total stored energy dissipated in a cavity evolves in time as

$$\frac{dU_s}{dt} = -2\alpha U_s, \tag{41}$$

or

$$U_s(t) = U_{s0} \exp(-2\alpha t). \tag{42}$$

In the forthcoming analysis it is necessary to study both the cases where the cavity is completely filled with material and where the cavity is partially filled. The power dissipated in a material that completely fills a cavity is

$$W_d = \int \frac{\sigma_d}{2}|E|^2 dV + \int \frac{\omega\mu''}{2}|H|^2 dV, \tag{43}$$

where σ_d is the effective conductivity of the dielectric, $\sigma_d = \omega\epsilon'' + \sigma$, and σ is defined by $\vec{J} = \sigma\vec{E}$.

The quality factor due to a dielectric that completely fills the cavity is used to define the loss tangent of the material under test

$$Q_s = \frac{\omega \text{ (average stored energy)}}{\text{power loss per cycle}} = \frac{\omega U_{sf}}{W_{df}} = \frac{\omega\epsilon_r'\epsilon_0}{\sigma_d} = \frac{1}{\tan\delta}, \tag{44}$$

where the subscript f refers to filled cavity. Generally, the materials under test will only partially fill the cavity. Since the dielectric does not completely fill the cavity, a correction must be applied. In what follows we outline the procedure for calculating the correction due to partial dielectric filling. The correction is obtained by considering losses in both the air-filled and dielectric-filled sections of the cavity separately.

The power dissipated in walls and end plates is given by integration of the Poynting vector over the surfaces [5]

$$W_w = \frac{R_s}{2}\int |H_\phi|^2 dS, \tag{45}$$

where the surface resistance is $R_s = \sqrt{\omega\mu'/2\sigma_w} = 1/d\sigma_w$, σ_w is the conductivity of the walls, and d is the effective penetration depth into the walls.

The total quality factor in the cavity is the ratio of energy stored in cavity and dielectric to power dissipated in walls, end plates, dielectric, and coupling ports

$$Q_t = \frac{\omega(U_{sd} + U_{sa})}{W_w + W_d + W_{cp}}, \tag{46}$$

where U_{sd} is the energy stored in the dielectric, U_{sa} is energy stored in air section of the cavity that contains a sample, and W_{cp} is the loss due to coupling ports. The coupling-port losses can be obtained by circle-fit procedures [6]. The quality factor without sample loss is Q_t'

$$Q_t' = \frac{\omega(U_{sd} + U_{sa})}{W_w + W_{cp}}. \tag{47}$$

In the nonmagnetic case, if we write $W_d = p\tan\delta$, where p is a parameter identified after performing the integration in eq (43) over the sample volume, then the net loss tangent can be calculated using eqs (46) and (47) given expressions for U_s, U_{sa}, W_w, and W_{cp} and eq (47). It can be put in the form

$$\tan\delta = \frac{p}{\omega(U_s + U_{sa})}\left(\frac{1}{Q_t} - \frac{1}{Q_t'}\right). \tag{48}$$

Q_t' is not directly measurable, however, a theoretical value for Q_t' can be calculated from eq (47), if the wall penetration depth is known. An estimate of wall penetration depth can be calculated from quality-factor measurement on the empty cavity:

$$Q_e = \frac{\omega U_e}{W_w + W_{cp}}\,; \tag{49}$$

therefore, the penetration depth is

$$d = \frac{\int_s |H_\phi|^2 dS}{2\sigma_w(\frac{\omega U_e}{Q_e} - W_{cp})}. \tag{50}$$

The calculated penetration depth can then be used in eq (47) for use in eq (48).

3.1. Wall Losses

Equation (45) yields the wall losses given the surface conductivity. The integrals can be calculated analytically on the outer walls, end plates, and inner conductor. The radial integration is slightly more complicated since the radial functions are not orthogonal.

The total wall loss is

$$\begin{aligned}
P_w &= \frac{R_s}{2}\int |H_\phi|^2 dS \\
&= \pi R_s[\sum_{m=0}^{\infty} B_{mm}^2 |A_{m(1)}\frac{j\omega\epsilon_1^*}{\sqrt{k_1^2-(m\pi/L)^2}}[J_1(\sqrt{k_1^2-(m\pi/L)^2}b) + Q_{1m}N_1(\sqrt{k_1^2-(m\pi/L)^2}b)]|^2 \\
&+ \sum_{m=0}^{\infty} B_{mm}^2 |A_{m(1)}\frac{j\omega\epsilon_1^*}{\sqrt{k_1^2-(m\pi/L)^2}}[J_1(\sqrt{k_1^2-(m\pi/L)^2}a) + Q_{1m}N_1(\sqrt{k_1^2-(m\pi/L)^2}a)]|^2 \\
&- \int_0^{d1} |\sum_{m=0}^{\infty} A_{m(1)}\frac{j\omega\epsilon_1^*}{\sqrt{k_1^2-(m\pi/L)^2}}[J_1(\sqrt{k_1^2-(m\pi/L)^2}a) + Q_{1m}N_1(\sqrt{k_1^2-(m\pi/L)^2}a)] \\
&\times \cos((d_2 - z)m\pi/L)|^2 dz \\
&+2\int_0^b \rho|\sum_{m=0,2,..} A_{m(1)}\frac{j\omega\epsilon_1^*}{\sqrt{k_1^2-(m\pi/L)^2}}[J_1(\sqrt{k_1^2-(m\pi/L)^2}\rho) + Q_{1m}N_1(\sqrt{k_1^2-(m\pi/L)^2}\rho)]|^2 d\rho \\
&+2\int_c^a \rho|\sum_{m=0,2,..} A_{m(2)}\frac{j\omega\epsilon_2^*}{\sqrt{k_2^2-(m\pi/L)^2}}[J_1(\sqrt{k_2^2-(m\pi/L)^2}\rho) + Q_{2m}N_1(\sqrt{k_2^2-(m\pi/L)^2}\rho)]|^2 d\rho \\
&+2\int_0^c \rho|\sum_{m=0,2,..} A_{m(3)}\frac{j\omega\epsilon_2^*}{\sqrt{k_3^2-(m\pi/L)^2}}J_1(\sqrt{k_3^2-(m\pi/L)^2}\rho)]|^2 d\rho].
\end{aligned} \tag{51}$$

The loss characteristics of various metals used in cavity construction are given in table 1.

Table 1: Conductivities of metals

Material	Conductivity, σ ($\times 10^7$ S/m)	Skin Depth, d (10 GHz) ($\times 10^{-7}$) m
Cu	5.80	6.60
Al	3.72	8.26
Ag	6.17	6.42
Au	4.10	7.85
70-30 brass	1.57	12.70

4. Measurements

Permittivity measurements were performed on a number of well-characterized materials. The results are given in table 2. Uncertainties were calculated by comparison with previous measurements of these materials. Numerical experimentation was performed on the convergence of the solution as a function of the number of TM_{0m} modes used in the expansions. 20 to 90 axial eigenfunctions in region 1 and 2 eigenfunctions in regions 2 and 3 were required for these measurements. Higher permittivity requires more expansion functions in region 3. Uncertainties are produced from a number of sources and will be analyzed in more detail in a future publication. Uncertainties for the measurements were calculated by a sensitivity analysis of sample thickness, resonant frequency, and quality factor. The small air gap between sample and electrodes produces a slightly lower measured permittivity. Corrections for the gap are summarized in [7]. The gap effects on the real part of the permittivity can be mitigated by electroplating sample surfaces with copper by applying conducting pastes, or by using tin foil with petroleum jelly as adhesive [8]. In the measurement of loss factor, gap mitigation methods will produce extraneous loss. Therefore,

Table 2: Dielectric measurements

Material	Frequency	Calculated (ϵ_r', ϵ_r'')
Crosslinked polystyrene	915 MHz	(2.524$\pm$ 0.020, 0.003$\pm$ 0.002)
Polytetrafluoroethylene	905 MHz	(2.072$\pm$ 0.020, 0.0025$\pm$ 0.002)
1723 Glass	840 MHz	(6.253$\pm$ 0.045 ,0.0217$\pm$ 0.003)

the loss measurement should be performed before the permittivity measurement.

5. Conclusions

The goal of this report was the development of the theory for the mode-matching solution for resonance in a reentrant cavity and the presentation of numerical results. The mode matching results in a determinantal equation. The roots of this equation yield the permittivity of the sample. A full-mode model for the cavity was developed and solved numerically. The solution allows accurate measurement of permittivity. Analytical expressions for wall losses were presented. The theoretical approach to characterization of the reentrant cavity was presented.

6. Acknowledgments

We thank Michael D. Janezic for help with software and David Hill for discussions.

References

[1] R.D. Harrington, R.C. Powell, and P.H. Haas, "A re-entrant cavity for measurement of complex permeability in the very-high frequency region," *J. Res. Nat. Bur. Stand. (U.S.)*, vol. 56, no. 3, pp. 129–133, 1956.

[2] C.N. Works, T.W. Dakin, and F.W. Boggs, "A resonant cavity method for measuring dielectric properties at ultra-high frequencies," *AIEE Trans.*, vol. 63, pp. 1092–1098, 1944.

[3] W. Xi, W.R. Tinga, W.A.G. Voss, and B.Q. Tian, "New results for coaxial re-entrant cavity with partially dielectric filled gap," *IEEE Trans. Microwave Theory Tech.*, vol. MTT-40, pp. 747–753, April 1992.

[4] R.J. Cook, *Microwave cavity methods*, pp. 12–27. IPC Science and Technology Press, 1973.

[5] J.D. Jackson, *Classical Electrodynamics*. New York: John Wiley and Sons, 1974.

[6] E.J. Vanzura, R.G. Geyer, and M.D. Janezic, "The NIST 60-millimeter diameter cylindrical cavity resonator: Performance evaluation for permittivity measurements," Natl. Inst. Stand. Technol., Tech. Note 1354, August 1993.

[7] J. Baker-Jarvis, "Transmission/reflection and short-circuit line permittivity measurements," Natl. Inst. Stand. Technol., Tech. Note 1341, July 1990.

[8] J.V.L. Parry, "Measurement of permittivity and power factor of dielectrics at frequencies from 300 to 600 Mc/s," *Proc. IRE*, vol. 98, pp. 303–311, 1951.

• U.S. GOVERNMENT PRINTING OFFICE 1996-0-573-018/40028

NIST *Technical Publications*

Periodical

Journal of Research of the National Institute of Standards and Technology—Reports NIST research and development in those disciplines of the physical and engineering sciences in which the Institute is active. These include physics, chemistry, engineering, mathematics, and computer sciences. Papers cover a broad range of subjects, with major emphasis on measurement methodology and the basic technology underlying standardization. Also included from time to time are survey articles on topics closely related to the Institute's technical and scientific programs. Issued six times a year.

Nonperiodicals

Monographs—Major contributions to the technical literature on various subjects related to the Institute's scientific and technical activities.

Handbooks—Recommended codes of engineering and industrial practice (including safety codes) developed in cooperation with interested industries, professional organizations, and regulatory bodies.

Special Publications—Include proceedings of conferences sponsored by NIST, NIST annual reports, and other special publications appropriate to this grouping such as wall charts, pocket cards, and bibliographies.

Applied Mathematics Series—Mathematical tables, manuals, and studies of special interest to physicists, engineers, chemists, biologists, mathematicians, computer programmers, and others engaged in scientific and technical work.

National Standard Reference Data Series—Provides quantitative data on the physical and chemical properties of materials, compiled from the world's literature and critically evaluated. Developed under a worldwide program coordinated by NIST under the authority of the National Standard Data Act (Public Law 90-396). NOTE: The Journal of Physical and Chemical Reference Data (JPCRD) is published bi-monthly for NIST by the American Chemical Society (ACS) and the American Institute of Physics (AIP). Subscriptions, reprints, and supplements are available from ACS, 1155 Sixteenth St., NW, Washington, DC 20056.

Building Science Series—Disseminates technical information developed at the Institute on building materials, components, systems, and whole structures. The series presents research results, test methods, and performance criteria related to the structural and environmental functions and the durability and safety characteristics of building elements and systems.

Technical Notes—Studies or reports which are complete in themselves but restrictive in their treatment of a subject. Analogous to monographs but not so comprehensive in scope or definitive in treatment of the subject area. Often serve as a vehicle for final reports of work performed at NIST under the sponsorship of other government agencies.

Voluntary Product Standards—Developed under procedures published by the Department of Commerce in Part 10, Title 15, of the Code of Federal Regulations. The standards establish nationally recognized requirements for products, and provide all concerned interests with a basis for common understanding of the characteristics of the products. NIST administers this program in support of the efforts of private-sector standardizing organizations.

Consumer Information Series—Practical information, based on NIST research and experience, covering areas of interest to the consumer. Easily understandable language and illustrations provide useful background knowledge for shopping in today's technological marketplace.

Order the **above** *NIST publications from: Superintendent of Documents, Government Printing Office, Washington, DC 20402.*

Order the **following** *NIST publications—FIPS and NISTIRs—from the National Technical Information Service, Springfield, VA 22161.*

Federal Information Processing Standards Publications (FIPS PUB)—Publications in this series collectively constitute the Federal Information Processing Standards Register. The Register serves as the official source of information in the Federal Government regarding standards issued by NIST pursuant to the Federal Property and Administrative Services Act of 1949 as amended, Public Law 89-306 (79 Stat. 1127), and as implemented by Executive Order 11717 (38 FR 12315, dated May 11, 1973) and Part 6 of Title 15 CFR (Code of Federal Regulations).

NIST Interagency Reports (NISTIR)—A special series of interim or final reports on work performed by NIST for outside sponsors (both government and non-government). In general, initial distribution is handled by the sponsor; public distribution is by the National Technical Information Service, Springfield, VA 22161, in paper copy or microfiche form.

U.S. Department of Commerce
National Institute of Standards and Technology
325 Broadway
Boulder, Colorado 80303-3328